Journal of Ceramic Processing Research. Vol. 17, No. 5, pp. 513~517 (2016)

J O U R N A L O F
Ceramic Processing Research

Chitosan assisted synthesis of $LiFePO_4$/Graphene/C composite and its electrochemical performance

Qiru Li, Zhufa Zhou*, Xingxing Zhang and ShanShan Liu
College of Chemistry, Chemical Engineering and Materials Science, Soochow University, Suzhou 215123, PR China

$LiFePO_4$/graphene/C composite was prepared using chitosan (CS) and graphene oxide (GO) as carbon sources via a facile solid state method. CS can bond with GO through electrostatic force between amino group on CS and carboxy group on GO. With high temperature treatment, GO can be reduced to graphene and CS can be decomposed into carbon. By adding chitosan, severe agglomeration of graphene can be prevented. As a result, a continuous conductive framework was formed. The good conductivity facilitates electron migration, contributing to excellent electrochemical performance especially the high-rate performance. Consequently, the composite $LiFePO_4$/graphene/C exhibited higher initial discharge capacity of 145.2 mAh · g^{-1} at the low rate of 0.1 C and retained 62.6 mAh · g^{-1} at high rate of 10 C, while the $LiFePO_4$ merely coated with graphene (LFP/G) was 125.9 mAh · g^{-1} (0.1 C) and 6.5 mAh · g^{-1} (10 C), respectively.

Key words: Lithium-ion batteries, $LiFePO_4$, Interconnected conductive network, High-rate performance.

Introduction

Since Goodenough proposed the olivine structured lithium transition-metal (ortho) phosphates, cathode materials like $LiFePO_4$, $LiMnPO_4$ and $LiCoPO_4$ had been extensively studied [1-4]. Though $LiMnPO_4$ possesses higher redox voltage plateau than $LiFePO_4$, lower conductivity and Jahn-teller effect seriously hamper its electrochemical performances [5]. The high redox potential of $LiCoPO_4$ will lead to the decomposition of the electrolyte during charge and discharge [6]. Therefore, $LiFePO_4$ becomes more suitable for energy storage application. Owing to the high capacity at a low rate and extraordinary thermal stability, $LiFePO_4$ has been applied in portable devices like mobile phones and laptops [7]. However, its intrinsic low electronic conductivity and small lithium ion diffusion coefficient impair its rate performance [8], hampering its potential application in high rate aspects like Electric Vehicles and Plug-in Hybrid Electric Vehicles [9].

Tremendous efforts have been devoted to overcome this problem, such as synthesis of nano-sized particles via vary methods like hydrothermal, solvothermal, sol-gel, co-precipitation and polyol [10-14], doping with cations like Mg^{2+}, Ti^{3+}, Ni^{2+} [15-17], coating with conductive materials [7, 18, 19]. It has been verified that carbon coating is a facile and efficient way to enhance the rate performance by increasing the electron transfer rate. Recently, graphene has aroused a great deal of attention. The distinctive structure endows it with many unique properties such as high specific surface area, outstanding electronic conductivity and superior mechanical characteristics [20]. This promising material has been applied in anode of lithium ion batteries [21], solar cells [22] and super capacitors [23]. Hitherto, some graphene coated cathode had also been reported. However, during the high-temperature treatment, graphene sheets are easily agglomerated, which will damage its electronic conductivity. And its 2D structure makes its contact with irregular pristine $LiFePO_4$ particles insufficient and loose, leading to unsatisfactory enhancement on electrochemical performances [24].

Chitosan (CS) is the second most abundant natural carbohydrate biopolymers with multiple functional groups like positive charged amino groups. Through electrostatic interaction, amino groups can interact with -COO^- group on GO [25].

Herein we report a facile method to prepare $LiFePO_4$ coated with graphene and carbon. It's worth pointing out that through high-temperature reaction, chitosan integrated oxide graphene can transform into graphene-carbon network via reduction of graphene oxide and carbonization of chitosan. By adding chitosan, severe agglomeration of graphene can be prevented. What's more, the carbon that derived from chitosan can offset the loose wrapping of graphene on the surface of $LiFePO_4$. As a result, the electronic conductivity of the bulk material can be enhanced.

Experimental

Synthesis

$LiFePO_4$/graphene/C composite with interconnected

*Corresponding author:
Tel : +86-0512-65880963
Fax: +86-0512-65880089
E-mail: zhouzhufa@suda.edu.cn

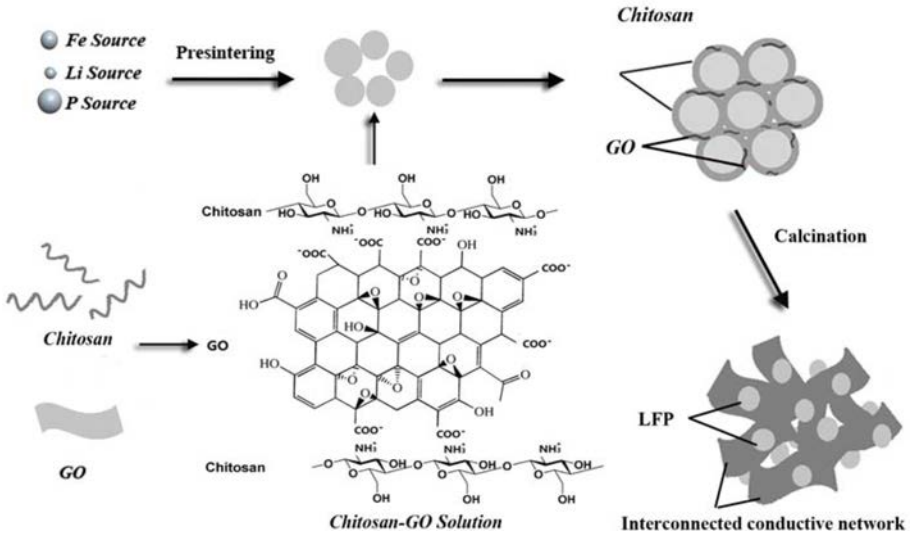

Fig. 1. Schematic illustration of the preparation process.

conductive network was prepared via a solid state method. Firstly, stoichiometric amount of Li_2CO_3, $FeC_2O_4 \cdot 2H_2O$ and $NH_4H_2PO_4$ were weighed and ball milled for 6 h using ethanol as medium. Then, the slurry was dried at 60 ºC and further treated in a furnace at 400 ºC for 10 h to get the precursor of $LiFePO_4$. Chitosan integrated graphene oxide was prepared as following: Chitosan was dissolved in 2% (v/v) acetic acid at room temperature. GO was prepared by modified Hummers' method. The as-prepared GO (5 wt. % of $LiFePO_4$) was added into chitosan solution (chitosan was 15 wt. % of $LiFePO_4$) with intensively stirring for 30 min to form a mixture. The precursor of $LiFePO_4$ were added into the mixture and grounded for 6 h. After being dried, the powder was put inside a crucible which was surrounded by granular activated carbon (Aldrich, 20-40 mesh). The powder was further calcined in a furnace at 750 ºC for 12 h. It is worth noting that the activated carbon used here produced a reductive atmosphere during high temperature treatment to avoid oxidation of Fe^{2+} and reduce the graphene oxide as well. The preparation procedure is shown in Fig. 1. $LiFePO_4$ particles solely coated with graphene (LFP/G) were also prepared using the same method.

Structural characterization and electrochemical test

The phase of the sample was characterized by X-ray diffraction (XRD, Phillips, PW1700, Cu Kα radiation, λ = 0.15406 nm). The surface morphology was observed by a scanning electronic microscope (SEM, Philips XL 300).

The electrochemical performances of the samples were evaluated using a CR2032 coin-type cell. The slurry was made by dispersing the active materials with PVDF and acetylene black with a weight ratio of 8 : 1 : 1 in N-methyl-2-pyrrolidinone. And then, the slurry was pasted on a current collector of Al foil by a blade and dried at 80 ºC for 10 h in a vacuum oven. After pressing compactly by a roller press machine and tableting, cathode electrode sheets were obtained. Prepared electrode sheets were further dried at 120 ºC in a vacuum oven for 12 h. The coin-type cells were assembled in a glove box filled with pure Ar (99.9995% purity). The electrolyte was prepared by dissolving 1M $LiPF_6$ into a mixture of ethylene carbonate, dimethyl carbonate and ethyl methyl carbonate (1 : 1 : 1, by weight). Li-foil and Celgard 2300 film were used as the anode electrode and separator, respectively.

The cells were galvanostatically charged and discharged at different currents (0.1 C, 1 C, 2 C, 5 C and 10 C) within the voltage range of 2.5 V-4.2 V on the electrochemical test instrument (CT2001A, Wuhan Land Electronic Co. Ltd., China) at room temperature. Electrochemical impedance spectroscopy (EIS) was carried out in a frequency range between 100 kHz and 10 mHz by the electrochemical work station (Shanghai Chenhua Instrument Co. Ltd., China).

Results and Discussion

Crystalline structure analysis

Fig. 2 shows the XRD patterns of LFP/G/C and LFP/G. The main diffraction peaks of all samples can be attributed to the orthorhombic $LiFePO_4$ olivine-type phase (JCPDS Cnard No. 40-1499) with high intensity. Obtained lattice constants for LFP/G/C are a = 10.289 Å, b = 6.017 Å, c = 4.692 Å, while values of LFP/G are a = 10.329 Å, b = 6.014 Å, c = 4.702 Å. These parameters agree fairly well with previous report [2]. No other peaks can be observed, which verify that the addition of graphene and carbon have no effect on the crystal structure.

The morphology of the LFP/G/C and LFP/G were observed by SEM. As shown in Fig. 3a, $LiFePO_4$

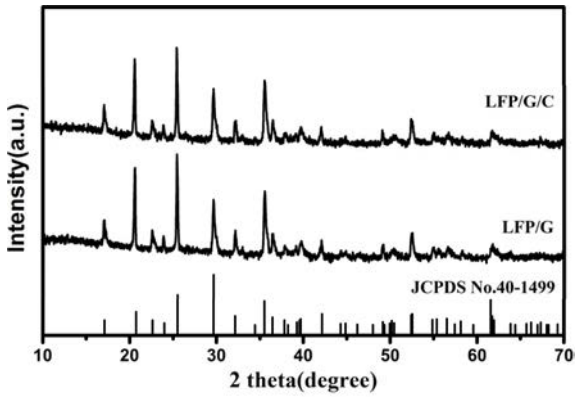

Fig. 2. X-ray diffraction patterns of LFP/G/C and LFP/G.

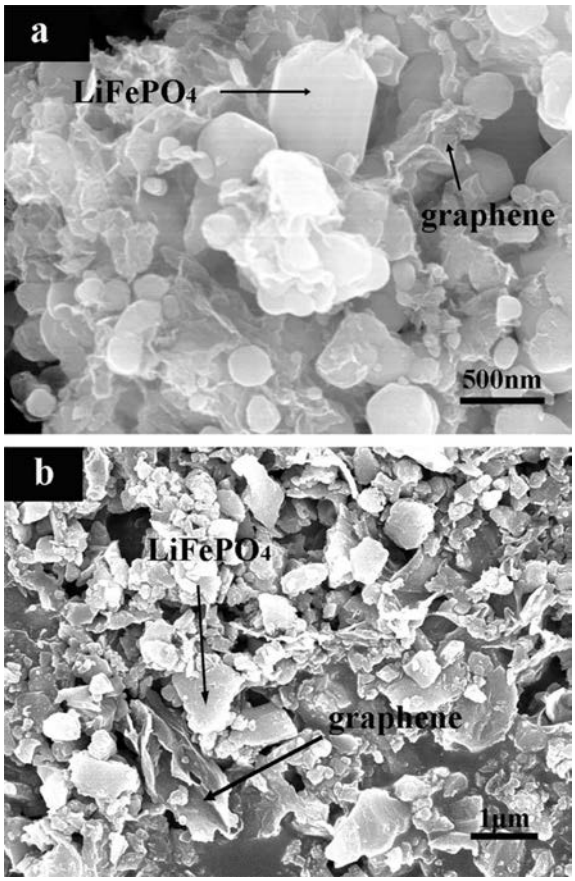

Fig. 3. SEM images of (a) LFP/G/C, (b) LFP/G.

particles of LFP/G/C exist mainly in the form of sphere. Among particles, sheets of graphene layers can be observed. The $LiFePO_4$ particles are well embedded in graphene network. The graphene layers of LFP/G (shown in Fig. 3b) tended to agglomerate and formed into thick and large layers. And the connection between graphene and irregular $LiFePO_4$ particles are loosely and insufficient. Comparing LFP/G/C with LFP/G, it could be concluded that the addition of chitosan can prevent graphene sheets forming into thick layers. The $LiFePO_4$ particles sizes of LFP/G are around 0.3-1 μm, while sizes of LFP/G/C are mainly about 100-500 nm.

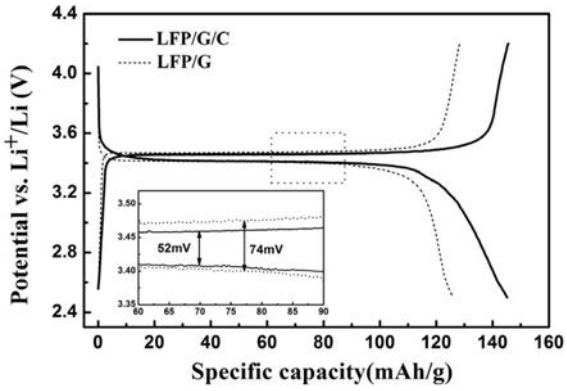

Fig. 4. The initial charge-discharge potential diagrams of LFP/G/C and LFP/G at the current density of 0.1 C.

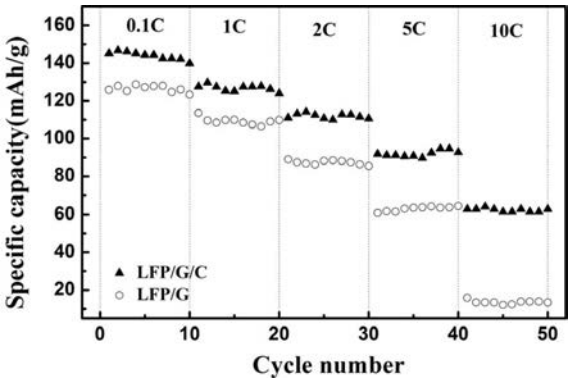

Fig. 5. Rate performance of LFP/G and LFP/C/G at 0.1 C, 1 C, 2 C, 5 C and 10 C for 10 cycles.

The obtained network can effectively isolate the $LiFePO_4$ particles and prevent the agglomeration of the particles, making the sizes much smaller.

Electrochemical performance

Fig. 4 shows the initial charge-discharge potential diagrams of LFP/G/C and LFP/G at 0.1 C.The voltage plateau over a wide voltage range approximately at 3.4 V (versus Li/Li^+) is the characteristic voltage plateau of $LiFePO_4$. The initial discharge capacities for the LFP/G/C and LFP/G samples at 0.1 C are 145.2 $mAh \cdot g^{-1}$ and 125.9 $mAh \cdot g^{-1}$, respectively. Although graphene has good electrical conductivity, insufficient and loosing contact with irregular pristine $LiFePO_4$ particles can't fully realize its excellent property. The high discharge capacity of chitosan prepared samples can be partly ascribed to larger surface of the small particles which can offer more active sites for electrochemical reactions between electrolyte and active materials. What's more, smaller particle size contributes to shorter diffusion length of lithium ions, which is beneficial for efficient transition between $FePO_4$ and $LiFePO_4$. The voltage difference between the charge and discharge platform reveals the polarization of the system. After co-modifying with carbon and graphene, the polarization between the charge and discharge plateau is reduced to 52 mV, while

Table 1. The discharge capacity of different cathodes at different rates (mAh • g^{-1}).

Cathode	0.1 C	1 C	2 C	5 C	10 C	Retention at 10 C (%)
LFP/G	125.9	109.2	87.3	42.2	6.5	5.2
LFP/G/C	145.2	126.8	111.9	92	62.6	43.1

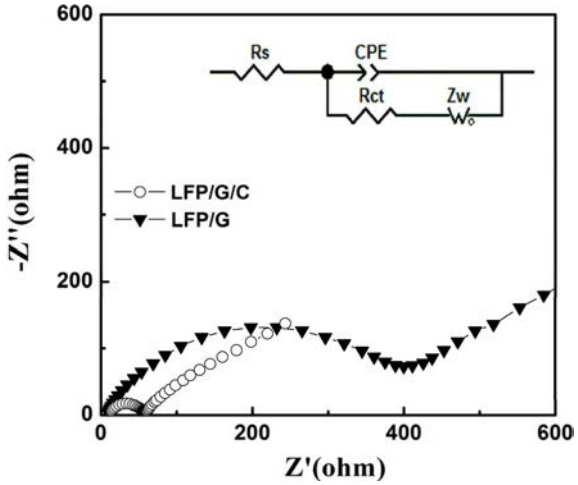

Fig. 6. Impedance spectra of LFP/G/C and LFP/G.

Table 2. Impedance parameters of the samples.

Sample	Rs (Ω)	Rct (Ω)
LFP/G	9.48	400.7
LFP/G/C	11.58	45.72

simply modified with graphene is 74 mV, indicating that the electrochemical kinetics of the $LiFePO_4$ can be improved due to interconnected conductive network.

Rate performances of all the samples are displayed on Fig. 5. The cells were cycled at 0.1 C, 1 C, 2 C, 5 C and 10 C for 10 cycles, respectively. Detailed discharge capacities at different rates are displayed in Table 1. Obviously, all the cells have relative high capacity at a low current rate of 0.1 C. However, gradual decline of discharge capacity occurred with increasing of the current rate. When rate was increased above 2 C, LFP/G suffered a sudden loss in capacity. Especially when the rate increased as high as 5 C, the discharge capacity of LFP/G began to dramatically degrade. The chart indicates that even experienced a rate of 10 C, the LFP/G/C still could maintain 43.11% capacity. This could be explained by the stable conductive network around $LiFePO_4$ particles. Though coated with carbon can minimize the particle size to a certain extent, decrease proportion of active material in the composite as well as the blocking of the diffusion path of lithium ion will lead to unexpected loss of the discharge capacity. While by combining graphene and carbon, the amount of conductive materials can decrease to a certain level and maintain the desire performances as well. EIS tests were employed to analyze the inner impedance of the electrodes. An equivalent circuit (shown in Fig. 6) was employed to explain the obtained EIS spectra. The impedance spectra consist of a semicircle in the high frequency region and a slope line in low frequency region. A constant phase element CPE was placed to represent the double layer capacitance and passivation film capacitance. Rs represents the resistance of electrolyte, corresponding to the intercept impedance on the real axis; Rct associates with the charge transfer resistance, corresponding to the semicircle in high frequency region; and Zw is the Warburg impedance related to the diffusion of Li ions into bulk materials, corresponding to the inclined line in the low-frequency range. Values of Rs and Rct of LFP/G/C and LFP/G composites were obtained from computer simulations using the Zview 2.0 software. The values of Rs and Rct of LFP/G and LFP/G/C are listed in Table 2.

The values of Rs are similar which is due to the same electrolyte we used in this study. Obviously, the Rct value of electrode prepared together with chitosan and graphene oxide was smaller, confirming the electronic conductivity of $LiFePO_4$ particles could be enhanced by conductivity network of carbon-graphene. These results are in good agreement with the differences in the rate performance of the electrodes.

Conclusions

The $LiFePO_4$ particles coated with combined conductive network were successfully prepared by a simple solid state method. The effects of carbon-graphene network on the electrochemical performance of cathode are investigated in this paper. The results show that carbon-graphene network can minimize the particle sizes and prevent the agglomeration of the graphene layers and $LiFePO_4$ particles as well. Continuous conductive network can facilitates electrons migration, thus contributing to the improvement of electrochemical performances especially the rate performance of the cathode. Compared with sample solely coated with graphene (LFP/G), LFP/C/G not only possessed higher discharge capacity at low rate of 0.1 C but also exhibited excellent high-rate performance of 62.6 mAh • g^1 at 10 C, while LFP/G had already faded.

Acknowledgments

This work was supported by the Priority Academic Program Development (PAPD) of Jiangsu Higher Education Institutions.

References

1. Padhi AK, Nanjundaswamy KS, Goodenough JB, J Electrochem Soc. 144 (1997) 1188-1194.
2. Jae-Kwang Kim, Crystengcomm. 16 (2014) 2818-2822.
3. M. Zhao, Y. Fu, N. Xu, G. R. Li, M.T. Wu and X. P. Gao, J. Mater. Chem. A 2 (2014) 15070-15077.

4. H. H. Li, Y.P. Wang, X.L. Yang, L. Liu, L. Chen and J. P. Wei, Solid State Ionics. 255 (2014) 84-88.
5. L. F. Zhang, Q. T. Qu, L. Zhang, J. Li and H. H. Zheng, J. Mater. Chem. A 2 (2014) 711-719 .
6. S. Theil, M. Fleischhammer, P. Axmann and M. Wohlfahrt-Mehrens, J. Power Sources 222 (2013) 72-78.
7. L. Y. Tan, Q. L. Tang, X. H. Chen, A. P. Hu, W. N. Deng, Y. S. Yang and L. S. Xu, Electrochim. Acta 137 (2014) 344-351.
8. Naik, J. Zhou, C. Gao, L. Wang, Electrochim. Acta 142 (2014) 215-222.
9. L. Tan, L. Zhang, Q. N. Sun, M. Shen, Q. T. Qu and H. H. Zheng, Electrochim. Acta 111 (2013) 802-808.
10. W. Yu, L. L. Wu, J.B. Zhao, Y. P. Zhang and G. Z. Li Adv. Powder Technol. 25 (2014) 1688-1692.
11. C. W. Sun, S. Rajasekhara, J. B. Goodenough and F. Zhou, J. Am. Chem. Soc. 133 (2011) 2132-2135.
12. D. Choi, P.N. Kumta, J. Power Sources 163 (2007) 1064-1609.
13. Y. Zhu, S. Z. Tang, H. H. Shi, H. L. Hu, Ceram. Int. 40 (2014) 2685-2690.
14. Vinod Mathew, M. H. Alfaruqi, J. Gim, J. Song, S. Kim, D. Ahn, and J. Kim, Mater. Charact. 89 (2014) 93-101.
15. X. Zhao, Dong-Ho Baek, Z. X. Wang, L. Wu, J. C. Zheng and H. J. Guo, Mater. Res. Bull. 47 (2012) 2819-2822.
16. L. Li, X. H. Li, Z. X. Wang, L. Wu, J. C. Zheng and H. J. Guo, J. Phys. Chem. Sol. 70 (2009) 238-242.
17. Y. C. Ge, X. D. Yan, J. L, X. F. Zhang, J. W. Wang, X. G. He, R. S. Wang and H. M. Xie, Electrochim. Acta 55 (2010) 5886-5890.
18. P.-Z. Gao, L. Wang, D.-Y. Li, B. Yan, W.-W. Gong, Ceram. Int. 40 (2014) 13009-13017.
19. A. Fedorková, A. Nacher-Alejos, P. Gomez-Romerob and et al, Electrochim. Acta 55 (2010) 943-947.
20. Engin Era and Hüseyin Çelikkan, RSC Adv. 4 (2014) 29173-29179.
21. X. Y. Zhou, J. Shi, Y. Liu, Q. M. Su, J. Zhang and G. H. Du, Electrochim. Acta 143 (2014) 175-179.
22. V.V. Brus, M.A. Gluba, X. Zhang, K. Hinrichs, J. Rappich, N.H. Nickel, Sol. Energy 107 (2014) 74-81.
23. R. Kumar, H.-J. Kim, S. Park, A. Srivastava, I.-K. Oh, Carbon 79 (2014) 192-202.
24. X. F. Zhou, F. Wang, Y. M. Zhu and Z. P. Liu, J. Mater. Chem. 21 (2011) 3353-3358.
25. S. Debnath, A. Maity, K. Pillay, J. Environ. Chem. Eng. 2 (2014) 963-973.